Cancer Science
The official journal of the Japanese Cancer Association

Angiostatic activity of human plasminogen fragments is highly dependent on glycosylation

Ivan Carlos Santos,[1] Vivian Nogueira Silbiger,[4] Débora Ayame Higuchi,[4] Maria Aparecida Gomes,[1] Lucíola Silva Barcelos,[1] Mauro Martins Teixeira,[1] Mirian Teresa Paz Lopes,[1] Valbert Nascimento Cardoso,[3] Mercia Paula Lima,[2] Ronaldo Carvalho Araujo,[5] João Bosco Pesquero[5] and Jorge Luiz Pesquero[1,6]

[1]Institute of Biological Sciences, [2]Nursing School, [3]Faculty of Pharmacy, Federal University of Minas Gerais, Belo Horizonte, Minas Gerais; [4]University of Mogi das Cruzes, [5]Federal University of São Paulo, São Paulo, Brazil

(Received June 20, 2009/Revised October 5, 2009/Accepted October 6, 2009/Online publication November 25, 2009)

To assess the importance of carbohydrate moieties to the anti-angiogenic activity of plasminogen fragments, we cloned the fragment corresponding to amino acids Val^{79} to Thr^{346} (Kint3–4) that presents the three glycosylation sites. The activity of glycosylated and unglycosylated Kint3–4 was tested in murine sponge implant model. We observed a significant decrease in the neovascularization on the sponge after treatment with Kint3–4 by histological examination and determination of the hemoglobin levels. The effects were more intense with the glycosylated than the unglycosylated protein. ^{99m}Technecium-labeled red blood cells confirmed the inhibition of cell infiltration in the implanted sponge. Studies using melanoma B16F1 implanted in a mouse demonstrated that treatment with glycosylated Kint3–4 (0.15 nmol/48 h) during 14 days suppresses tumor growth by 80%. The vascular endothelial growth factor mRNA levels on the tumor were reduced after treatment. Kint3–4 is a potent plasminogen fragment that has been found to inhibit tumor growth. (*Cancer Sci* 2010; 101: 453–459)

The vasculature is an important organ. Angiogenesis, the formation of new blood vessels from pre-existing capillaries, is a fundamental and complex process involved in reproduction, cellular development, and pathological events, such as inflammation, diabetic retinopathy, endometriosis, adiposity, and cancer.[1,2] During tumor growth and chronic inflammation, neovascularization is required for the provision of nutrients and oxygen and to mobilize host cells, such as leukocytes.[3,4] The new vascular network demands an extensive interplay between cells, soluble factors, and extracellular components, and is tightly regulated by the expression of angiogenic and angiostatic factors.[5,6] A wide range of molecules mediates angiogenesis by acting directly or indirectly on endothelial cells via accessory cells, such as polymorphonuclear leukocytes.[7–9] Among these molecules are fragments of the plasmatic glycoprotein plasminogen, which have different angiostatic activity. Plasminogen presents five segments that, because of their specific structure, were designated as kringles (K1–K5). The antiproliferative activity of plasminogen is shared by K1, K2, K3, and K4 being the most potent angiostatin (K1–4 corresponding to amino acids Cys^{84}–Cys^{435}), followed by K2–3.[10,11] The sequence numbering of plasminogen starts with Glu^{1} of the mature protein or Glu^{20} for human plasminogen when including signal peptide. K2 and K3 individually or in combination exhibit weak activity when compared with K2–3, and a combination of K1–3 and K4 resulted in the same activity level of K1–4.[11] It was also observed that the most potent inhibitor of endothelial cell angiogenesis of is K1–3 (amino acids Cys^{84}–Cys^{333} of plasminogen).[12] These results show that proteolytic processing with the exposure of anti-angiogenic sites, kringle conformation, interkringle interaction, and carbohydrate moieties can alter efficiency and function. Despite the anti-angiogenic activity of kringles, the importance of carbohydrates is poorly understood. Angiostatin expressed in *Pichia pastoris* (*P. pastoris*) potently inhibited Lewis lung cancer and a B16–BL6 experimental metastasis model at a similar potency of angiostatin and K1–3 expressed in Chinese hamster ovary (CHO) cells.[12] The half-life of proteins expressed in *P. pastoris* was sevenfold lower than those expressed in CHO.[12] The authors attributed this effect upon half-life to any mammalian processing advantage, such as glycosylation. In mice, the endogenous angiostatin has a long half-life in circulation (greater than 2 days), but the native human angiostatin has a considerably shorter half-life of 4 h.[13] There is some controversy in the literature regarding the capacity of *P. pastoris* to modify a protein by glycosylation. While some authors verified that most proteins are modified by N-linked glycosylation of the high-mannose type, and virtually none are modified by O-linked glycosylation,[14] others found that the major products are O-linked mannose, and in the case of plasminogen, only a very small quantity of N-linked oligosaccharides is present on Asn^{289}.[15] The present study was developed to address the importance of carbohydrates for the biological activity of plasminogen fragments. One recombinant protein, Kint3–4, was produced using *P. pastoris.* Kint3–4 contains amino acids Val^{79}–Thr^{346} and the three glycosylation sites of plasminogen. Kint3–4 corresponds to the K1–3 fragment of human plasminogen extended 13 amino acids in the direction of K4. In addition, the protein presents fusion between Val^{79} and eight amino acids (EAEAYVEF) from the AOX1 signal peptide. The angiostatic activity of glycosylated and N-deglycosylated Kint3–4 was investigated by determination of its effect upon tumor growth and the inflammatory processes. Our results show that this C-terminal extension, with the inclusion of the third carbohydrate branch, improved the angiostatic activity and the half-life of the recombinant protein when compared to the potency of K1–3 expressed in CHO.[12] The removal of N-linked carbohydrates produced a much less efficient protein regarding capacity to inhibit tumor growth and vascularization.

Materials and Methods

Animals. Eight-week-old, male C-57 mice (25–30 g) were obtained from Animal Facilities of Federal University of Minas Gerais (Belo Horizonte, Brazil). After sponge (or tumor) implantation, the animals were maintained in individual cages with food/water ad libitum and in a controlled environment (temperature and humidity). The experiments were done within the guidelines established by the Brazilian College for Animal Experimentation and by the local animal ethics committee. B16F1 murine melanoma cells were from Ludwig Cancer Research Institute (São Paulo, Brazil).

[6]To whom correspondence should be addressed.
E-mail: jlpesq@icb.ufmg.br

doi: 10.1111/j.1349-7006.2009.01403.x

Cloning and transformation of *Pichia pastoris*. The fragment encoding amino acids 79–346 of human plasminogen was amplified from a cDNA library (Helica Biosystems, Helica, Fullerton, CA, USA) using the primers GAATTCGTGTA TCTCTCAGAGTGC and GCGGCCGCTTATGTGGGAGCCA ATTG. The polymerase chain reaction (PCR) product was cloned into pGEM-T (Promega, Madison, WI, USA) and subcloned into pPIC9 (Invitrogen, Carlsbad, CA, USA) at the *Eco*RI and *Not*I sites. pPIC9 containing the insert was linearized by using *Bgl*II and the product was fused to transform the *P. pastoris* strain SMD1165. Positive clones were identified by replica plating of colonies in methanol.

Fermentation and purification. Positive clones were grown into a 1-L flask containing 150 mL of yeast extract-peptone-dextrose (YPD) medium. The samples were incubated at 30°C, 240 rpm for 14 h. At optical density 2–6, the entire volume of inoculum was transferred to a 14-L fermentor vessel (Bioflo 110; New Brunswick Scientific, Edison, NJ, USA) containing 3 L basal salt medium plus 4.4 mL/L PTM1 trace metal solution and glycerol (40 g/L).[16] The temperature was controlled at 30°C. The dissolved oxygen set point was 30%, and pH was set at 5 and automatically adjusted with 7% ammonium hydroxide. After 20 h fermentation, the glycerol-fed batch process was initiated. The feeding medium consisted of 50% glycerol supplemented with 12 mL/L trace metal solution. The feed rate was 24 mL/L/h [16] until the biomass reached 200 g/L when the induction phase was started. The induction medium consisted of 100% methanol supplemented with 12 mL/L trace metal solution. The feeding was divided into three stages: 24-h induction with 1 mL/L/h; 24–48-h induction with 2 mL/L/h; and 48–72-h induction with 3 mL/L/h. The recombinant protein was purified by a process involving tangential filtration at the first step in a hollow-fiber system using a 5-kDa cut-off membrane to separate low molecular mass contaminants. The protein from the hollow-fiber system was loaded in a gel filtration column (Sephadex G100, 2.5 × 60 cm; Pharmacia, Upsala, Sweden) eluted with 0.1 M sodium phosphate buffer, pH 7.0. Partially-purified recombinant Kint3–4 (300 μg) was loaded on a Sephasil (C8) reverse-phase column (Pharmacia Biotech, Pharmacia, Upsala, Sweden) eluted with a linear gradient from 0% to 100% acetonitrile containing 0.1% trifluoroacetic acid (TFA).

Deglycosylation. The tubes containing the protein eluted from the reverse-phase column were dried and then resuspended into 20 μL water. Ten micrograms of protein were solubilized in 20 μL denatured solution (5% sodium dodecyl sulfate [SDS] and 10% β-mercaptoethanol) and boiled for 10 min. After boiling, 1 μL of 50 mM sodium phosphate buffer (pH 7.5), 1 μL of 10% Nonidet P-40, and 1 μL of 500 U peptide-N-glycosidase F (PNGase F; New England Biolabs, Ipswich, MA, USA) were added and incubated at 37°C for 24 h. The product of incubation was loaded on 10% SDS–polyacrylamide gel electrophoresis. For the biological assays, the deglycosylated protein was previously submitted to a filtration process through a 10-kDa membrane (Amicon; Millipore, Billerica, MA, USA) to remove carbohydrates.

Angiogenesis in sponge disc implants. Angiogenesis was indirectly determined by the sponge implant model in mice.[17] Polyurethane sponge discs (Vitafoam, London, UK), 8 mm in diameter and 5 mm thick, were used as the matrix for fibrovascular tissue growth. The sponge discs were sterilized overnight in 70% ethanol and by boiling in distilled water for 15 min before the implantation. The animals were anesthetized by an intraperitoneal injection of 2.5% tribromoethanol (Sigma Chemical, St Louis, MO, USA) 1 mL/100 g body weight. The sponge discs were aseptically implanted into a subcutaneous pouch. The animals with the implant were randomly divided into two groups ($n = 6$ each group). Treatment was initiated 24 h after the implantation with subcutaneous daily injections of purified Kint3–4 (0.5, 5, or 50 μg per animal per day) or deglycosylated Kint3–4 (0.5, 5, or 50 μg per animal per day). The control group received daily injections of 100 μL of 0.9% saline. On day 11 from the initiation of treatment (10 doses), the implanted mice were anesthetized by an intraperitoneal injection of tribromoethanol and killed by cervical dislocation. The sponge was removed, dissected from the adherent tissue, weighed, and homogenized for hemoglobin quantitation. Alternatively, the sponges were analyzed for histological assessment.

Histology. The sponge implants were fixed in 10% formalin ($n = 3$, prepared in isotonic saline) and embedded in paraffin; 5 μm-thick sections were obtained. The sections were stained with hematoxylin–eosin and examined under a light microscope.

Tumor growth. The B16F1 melanoma cells were cultivated in RPMI-1640 medium with 5% fetal bovine serum. Cultures were kept at 37°C in a humidified, dark chamber (2.5% CO_2). After growth phase, the inoculum (5×10^5 cells) was prepared in saline and then injected subcutaneously into the mice. The treatment began 24 h after tumor implantation. Groups of 20 mice each were treated with three different doses of purified Kint3–4 (0.015 nmol [0.5 μg]/48 h, 0.15 nmol [5 μg]/48 h, or 1.5 nmol [50 μg]/48 h or purified deglycosylated Kint3–4 (0.47 nmol [0.5 μg]/48 h, 4.7 nmol [5 μg]/48 h, or 47 nmol [50 μg]/48 h) or 50 μg protein from fermentation without methanol induction. The samples were administered subcutaneously until day 14 (7 doses), and on day 15, the animals were killed and the tumor removed and weighed. The control group received injections of 100 μL of 0.9% saline.

Hemoglobin measurement. *Colorimetric.* One-hundred milligrams of the sponge implant or tumor were excised, homogenized in 2 mL Drabkin reagent (Labtest, Lagoa Santa, MG, Brazil), and centrifuged at 10 000*g* for 15 min. The supernatant was filtered through a 0.22-μm filter (Millipore, Billerica, MA, USA), and the hemoglobin in the sample was determined at 540 nm. The amount of hemoglobin was calculated from known amounts used as standards assayed in parallel.[18,19] The results were expressed as μg Hb/mg of wet tissue.

^{99m}Technecium (Tc)-labeled red blood cells. The procedure used was as previously described.[20] The heparinized blood of the mice (2 mL) was incubated with 1 mL $SnCl_2$ (2.4 μg/mL) for 60 min at 37°C, followed by incubation for 10 min at 37°C with 0.5 mL of ^{99m}Tc (1 mCi). The solution was centrifuged for 10 min at 2500*g* and the pellet resuspended in 2 mL saline (procedure repeated three times). ^{99m}Tc-labeled red blood cells (250 μL) were injected into the caudal vein of the mice. After 5 min, the animals were killed by cervical dislocation, the sponges removed, weighed, and gamma radiation was counted (ANSR-Abbott, Chicago, IL, USA).

Myeloperoxidase activity. The quantification of neutrophil tissue accumulation was indirectly determined by myeloperoxidase (MPO) activity.[21] The reaction mixture (150 μL) contained 1.6 mM 3,3′–5,5′-tetramethylbenzidine (TMB; Sigma, St Louis, MO, USA) dissolved in dimethylsulfoxide (Merck, Darmstadt, Germany), 0.003% H_2O_2 dissolved in 0.05 M phosphate buffer (0.5% HETAB, pH 5.4), and 25 μL supernatant from the tissue sample. The reaction was run for 5 min at 37°C in a 96 well microplate and was started by adding the supernatant and the TMB solution. After that, H_2O_2 was re-added and the mixture was incubated at 37°C for 5 min. The reaction was stopped by adding 100 μL of 4 M H_2SO_4 and the products were quantified at 450 nm. The neutrophil content was calculated from a standard curve based on MPO activity expressed as absorbance increase at 450 nm from 5% casein peritoneal-induced neutrophils assayed in parallel. The results are expressed as the relative number of neutrophils per milligram of wet tissue.

***N*-acetylglucosaminidase activity.** Quantification of macrophage tissue accumulation was indirectly determined by *N*-acetylglucosaminidase (NAG) activity.[21] The reaction mixture

doi: 10.1111/j.1349-7006.2009.01403.x

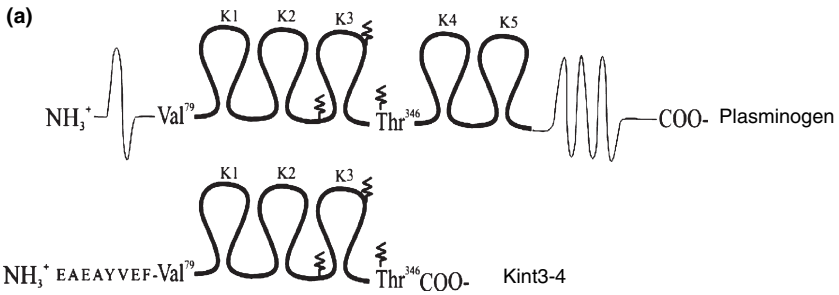

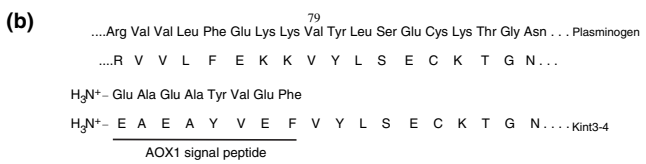

Fig. 1. (a) Schematic drawing of plasminogen and Kint3–4 molecules showing the kringles (K) and the carbohydrates moieties (ϟ). EAEAYVEF, fused sequence from the AOX1 signal peptide. (b), Partial amino-terminal sequence of plasminogen and recombinant Kint3–4. The amino acids Val^{79} and Thr^{346} are identified.

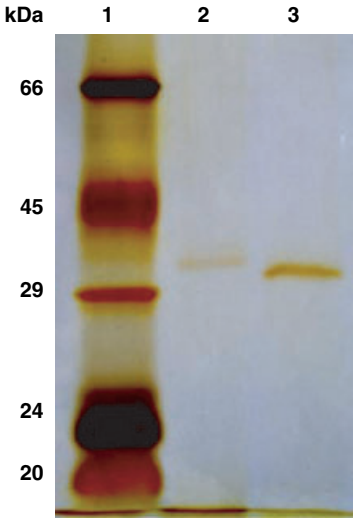

Fig. 2. Sodium dodecylsulfate–polyacrylamide gel electrophoresis (10%) of Kint3–4 expressed by *Pichia pastoris*. Lane 1, standard molecular weight; lane 2, purified recombinant Kint3–4; lane 3, purified recombinant Kint3–4 after digestion with peptide-N-glycosidase F.

(200 μL) contained 2.24 mM *p*-nitrophenyl-N-acetyl-β-D-glucosaminide (Sigma, USA) dissolved in citrate/phosphate buffer (0.1 M citric acid and 0.1 M Na_2HPO_4, pH adjusted to 4.5) and 100 μL supernatant from the tissue sample diluted in citrate/phosphate buffer. The reaction was run for 10 min at 37°C. The reaction was stopped by the addition of 100 μL of 0.2 M glycine buffer (pH 10.6) and the products quantified at 405 nm. The macrophage content was calculated from a standard curve based on NAG activity expressed as the absorbance increase at 405 nm from 3% thioglycollate peritoneal-induced macrophages assayed in parallel. The results are expressed in relative number of macrophages per milligram of wet tissue.

Vascular endothelial growth factor expression levels. Quantitative real-time PCR (qPCR) was performed with an ABI Prism 7000 Sequence Detection System (Applied Biosystems, Framingham, MA, USA) using Sybr Green detection. The final PCR mixture contained 1.5 μL each of forward and reverse primers (final concentration: 1.5 pmol each). β-Actin was used as an internal control to normalize the RNA amount used in the assay. The primers used were CGAGGCCCAGAGCAAGAGAG and GATCTTCTCCATGTCGTCCC (for mouse β-actin amplicon target of 87 bp), and AGTACATCTTCAAGCCGTCCTGTG and TCTGACGTGGGCACGCACTCC (for vascular endothelial growth factor [VEGF] amplicon target of 87 bp), 2 μL cDNA (4 μg), 10 μL SYBR PCR mix, and 5 μL pure PCR water in a 20 μL final volume. The reaction took place under universal cycling conditions, as specified by ABI (2 min at 50°C, 10 min at 95°C, 40 cycles of 15 s at 95°C, and 1 min at 60°C). Cycle threshold (CT) values were determined by automated threshold analysis with ABI Prism version 1.0 software (Applied Biosystems). The amplification efficiencies were determined by the slope of the dilution curve and linear regression (r^2) values. The expression level values of VEGF cDNA were given in nanograms using the CT values of the standard curve dilution.

Statistical analysis. Results are presented as mean ± SEM. Comparisons between groups were carried out using Student's *t*-test for unpaired data. For three or more groups, comparisons were carried out using one-way ANOVA, and differences between groups were assessed using an appropriate post-test test (as indicated). A *P*-value less than 0.05 was considered significant.

Results

Protein expression, sequencing and deglycosylation. The fragment of human plasminogen Kint3–4 (Fig. 1a) was expressed at very high levels (200 mg/L) by methylotrophic yeast *P. pastoris*. N-terminal sequencing of Kint3–4 at the N-terminus showed fusion between Val^{79} and the eight amino acids (EAEAYVEF) from the AOX1 signal peptide (Fig. 1b).

Kint3–4 was purified and presented a molecular mass of 34 kDa. To evaluate the importance of glycosylation in Kint3–4 activity, Kint3–4 was digested with PNGase F, which is specific for N-linked carbohydrates. After deglycosylation, carbohydrates were removed by ultra filtration through a 10-kDa membrane (Amicon; Millipore, Billerica, MA, USA). Deglycosylation caused the Mr 34 kDa band to migrate at Mr 32 kDa (Fig. 2).

Inflammatory angiogenesis in sponge implants. Angiogenesis and leukocyte influx was evaluated at day 11 after the beginning of treatment. The histological examination of the sponge sections showed decreased neovascularization when the animals were treated with glycosylated Kint3–4 at 50 μg/day compared to treatment with saline (Fig. 3). The vascularization level after treatment with 5 μg/day was not different to that observed for the control (data not shown). Neovascularization was also measured by evaluating the amount of hemoglobin within the

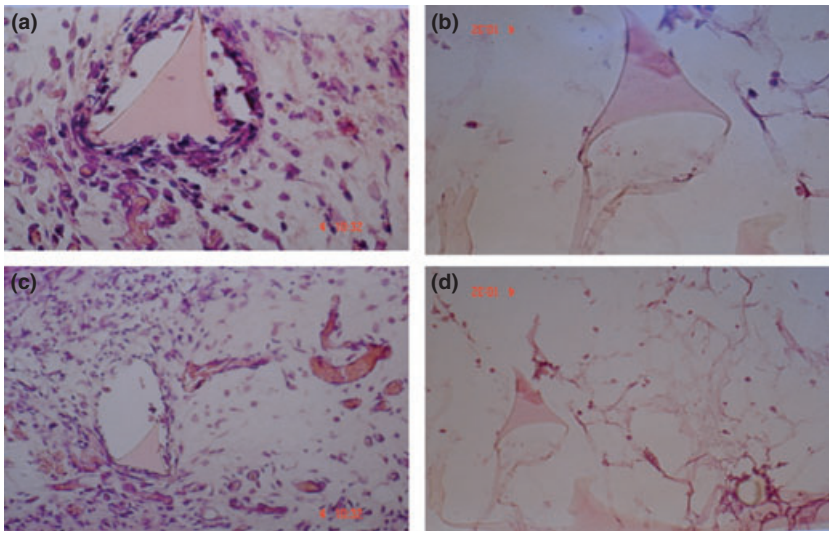

Fig. 3. Stained histological sections of implanted sponge evaluated on day 11 after the beginning of the treatment of mice with 5 μg/day glycosylated Kint3–4 (b,d, $n = 3$) and the control (a,c, $n = 3$) show the fibrovascular tissue infiltration pattern. Magnification ×40 (a,b) and ×20 (c,d).

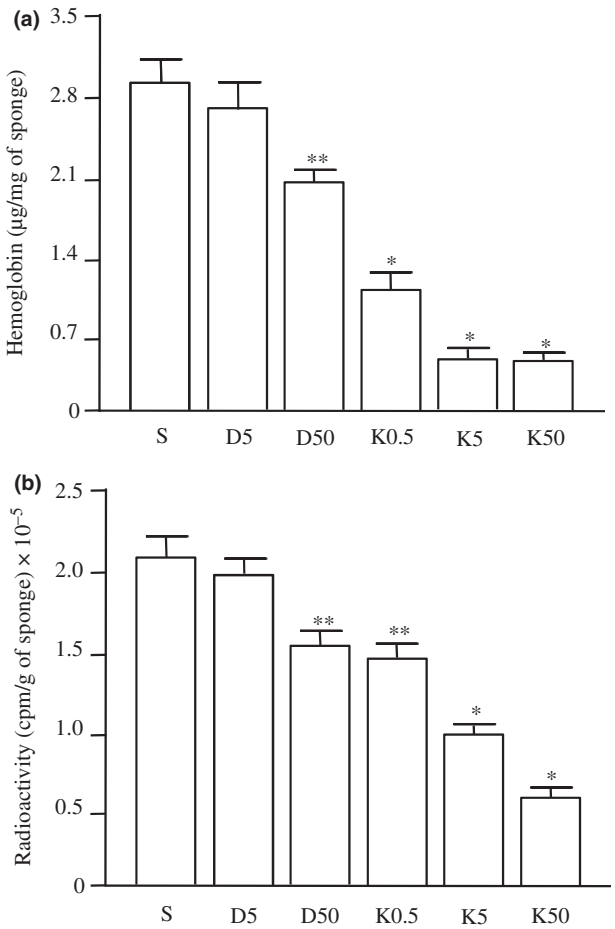

Fig. 4. Angiogenesis level in implanted sponge evaluated on day 11 after the beginning of the treatment with Kint3–4 (glycosylated or unglycosylated) or saline (S, control). Unglycosylated Kint3–4 at doses 5 (D5) or 50 (D50) μg/day; NI, non-induced fermentation; glycosylated Kint3–4 at doses 0.5 (K0.5), 5 (K5) or 50 (K50) μg/day. (a) Hemoglobin levels determined colorimetrically and expressed as microgram per milligram of wet weight of sponge. (b) ^{99m}Technecium-labeled red blood cells determined by radioactivity. Results represent the mean ± SEM of 5–7 animals for each group. *$P < 0.05$ *vs* control (C). Cpm, counts per minute.

sponge. There was a significant decrease (~60%) in the hemoglobin levels in the sponge of the animals treated with 0.5 μg/day glycosylated Kint3–4, and at 5 μg/day the decrease was approximately 80% (Fig. 4a). The effect of unglycosylated Kint3–4 was significantly lower (Fig 4a). ^{99m}Tc-labeled red blood cells confirmed the inhibition of cell infiltration by Kint3–4 (Fig. 4b).

Using MPO- and NAG-based assays, we observed a small effect in the accumulation of neutrophils and macrophages in the sponge (decrease of 20%–25%) with an injection of the unglycosylated protein at a dose of 50 μg/day (Fig 5). However, the injection of glycosylated Kint3–4 at dose of 0.5 μg/day or 5 μg/day led to a significant decrease (50% or 70%, respectively) in the accumulation of these cells (Fig. 5).

Tumor growth. Tumor mass was evaluated on day 15 after the beginning of treatment. Saline administration or 5 μg/48 h protein from non-induced fermentation did not inhibit tumor growth (Fig. 6). The administration of 50 μg/48 h (1500 μg/kg/48 h) unglycosylated protein inhibited tumor growth by 30%. For the glycosylated protein, the administration of 4.4 nmol (5 μg)/48 h (150 μg/kg/48 h) significantly inhibited the growth of experimental melanoma B16F1 by more than 80% as compared to the control (saline) (Fig. 6). The levels of VEGF mRNA on the implanted tumor melanoma B16F1, determined by real time PCR, decreased after treatment with Kint3–4. Standard curves ranging from 1 to 10^{-9} ng for both VEGF and β-actin cDNA demonstrated high linearity ($r^2 = 0.990$) with slopes smaller than −2 and calculated efficiencies ($E = -1/\text{slope}$) for both amplification reactions of 100%. The expression levels of the VEGF gene was given as absolute quantities of each VEGF amplicon normalized by its respective absolute β-actin quantity (ng of VEGF/ng of β-actin). The results of the absolute mean values are shown in Table 1. The qPCR detected was as low as 3.5×10^{-6} ng for VEGF cDNA in the tumor sample. The VEGF expression was significantly lower ($P < 0.05$) in the tumor sample from the animals treated with 50 μg/48 h of unglycosylated Kint3–4 than in the samples from animals treated with saline (1.94-fold lower than that of the control). However, treatment with glycosylated Kint3–4 produced a more intense effect upon tumor VEGF levels (K0.5: 2.04-fold lower than that of the control [$P < 0.05$]; K5: 4.17-fold lower than that of the control [$P < 0.01$]). No significant differences of the VEGF expression were observed in the tumor sample from the animals treated with non-induced fermentation or with 5 μg/48 h unglycosylated Kint3–4.

doi: 10.1111/j.1349-7006.2009.01403.x

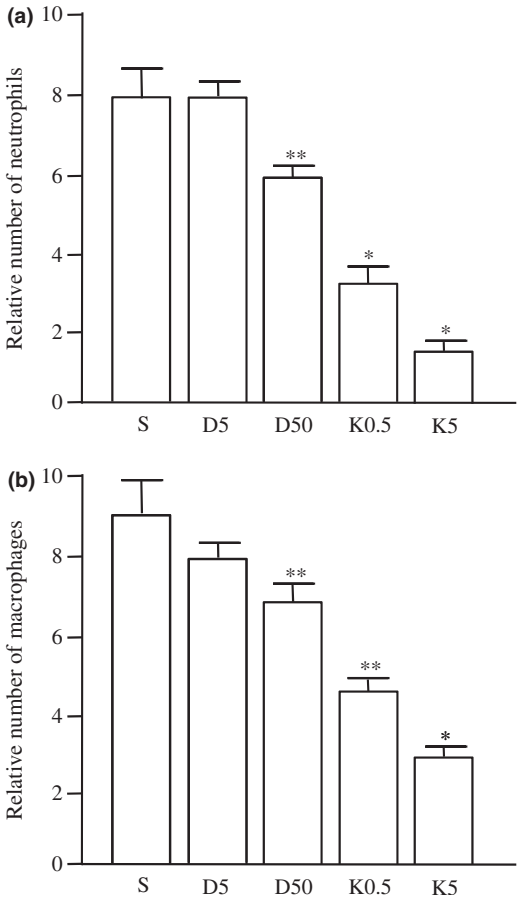

Fig. 5. Neutrophil (a) and macrophage (b) accumulation in the sponge in day 11 after beginning of treatment with systemically-injected Kint3–4 (glycosylated or unglycosylated) or saline (S, control). Unglycosylated Kint3–4 at doses 5 (D5) or 50 (D50) μg/day; NI, non-induced fermentation; glycosylated Kint3–4 at doses 0.5 (K0.5) or 5 (K5) μg/day. The recruitment of neutrophils or macrophages was evaluated by measuring myeloperoxidase and *N*-acetylglucosaminidase activities, respectively. Results represent the relative number of neutrophils ($\times 10^4$) or macrophages ($\times 10^4$) per milligram of wet tissue and are expressed by the mean ± SEM of 5–7 animals for each group. $^*P < 0.01$ *vs* control (saline) and $^{**}P < 0.05$ *vs* control (saline).

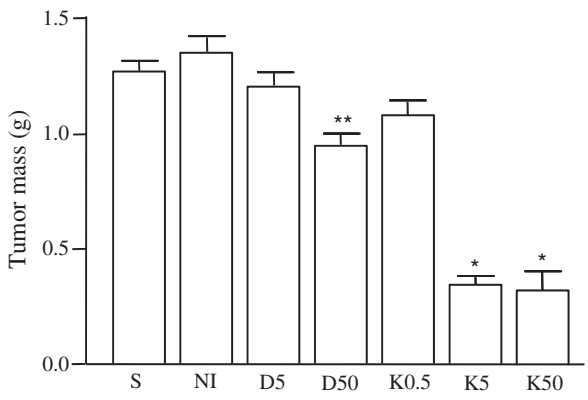

Fig. 6. Tumor mass evaluated on day 15 after the beginning of the treatment of animals with implanted melanoma. S, 0.9% saline; unglycosylated Kint3–4 at doses 5 (D5) or 50 (D50) μg/48 h; NI, non-induced fermentation; glycosylated Kint3-4 at doses 0.5 (K0.5), 5 (K5) or 50 (K50) μg/48 h. Results represent mean ± SEM of eight animals for each group. $^*P < 0.01$ *vs* control (saline) and $^{**}P < 0.05$ *vs* control (saline).

Table 1. Levels of transcript absolute expression of vascular endothelial growth factor (VEGF) from the tumor after treatment of tumor-bearing mice normalized to the invariant housekeeping gene β-actin

Sample	VEGF (ng)	β-Actin (ng)	VEGF/β-actin
Saline	$2.71 \pm \times 10^{-06}$	$7.61 \pm \times 10^{-04}$	0.00356
NI	$2.80 \pm \times 10^{-06}$	$7.40 \pm \times 10^{-04}$	0.00378
D5	$2.23 \pm \times 10^{-06}$	$6.67 \pm \times 10^{-04}$	0.00334
D50	$4.85 \pm \times 10^{-06}$	$7.01 \pm \times 10^{-04}$	0.00692*
K0.5	$5.67 \pm \times 10^{-06}$	$7.82 \pm \times 10^{-04}$	0.00725*
K5	$1.17 \pm \times 10^{-05}$	$7.88 \pm \times 10^{-04}$	0.01480**

Values are mean for each sample group ($n = 4$). Levels of transcripts determined in the tumor homogenate day 11 after the beginning of the treatment with saline (S, control), unglycosylated Kint3–4 at doses 5 (D5) or 50 (D50) μg/48 h; NI, non-induced fermentation; glycosylated Kint3–4 at doses 0.5 (K0.5) or 5 (K5) μg/48 h. $^*P < 0.05$ *vs* control (saline) and $^{**}P < 0.01$ *vs* control (saline).

Discussion

Since the early 1970s, when angiogenesis was recognized as a therapeutic and interesting tool,[22] there was been a greater increase in the knowledge of the pathways involved in this complex process. [23] Today, there are many anti-angiogenic substances undergoing clinical trials worldwide[24]. Among them is angiostatin, an internal fragment of plasminogen corresponding to the first four kringles.[13] Recombinant angiostatin systemically administrated at 1.5 mg/kg/day has been found to suppress the metastases of Lewis lung carcinoma, a low-metastatic phenotype tumor in mice, and at a dose of 100 mg/kg/day, suppresses the growth of the primary tumor.[25] At this dose, recombinant angiostatin administered daily has also been found to inhibit the growth of B16 murine melanoma by 90%.[26] However, such doses are very high to use in human therapy. Anti-angiogenic protein therapy includes repeated injections for long periods of treatment. As the production of functional recombinant proteins has been proven to be difficult, alternative approaches need to be developed in order to make the anti-angiogenic therapy viable. Kint3–4 improve the efficiency of anti-angiogenic therapy of plasminogen fragments and represent potential viability to be used in clinical settings. Our results showed that purified Kint3–4 at a lower dose (0.15 mg/kg/48 h) acts on tumors and reduce the tumoral mass by around 80%. Our results show also that *N*-deglycosylation of Kint3–4 produced a much less active protein in its ability to inhibit tumor growth and vascularization. The presence of the three carbohydrate moieties can be important for total activity. However, Kint3–4 is much more active than angiostatin, which can also present the three carbohydrates moieties. We believe two explanations are possible: (i) the glycosylation status as a result of *Pichia* glycosylation and protein manipulation; and (ii) the presence of the C-terminal segment of angiostatin that could impair its interaction by altering folding and stability. Plasminogen derived from plasma contains both O- and N-linked carbohydrates.[27,28] The O-linked carbohydrate could occupy two sites on plasminogens Ser^{249} and Thr^{346}, and the N-linked carbohydrate could occupy a site on Asn^{289}.[28] The presence of glycosylation can alter the properties of proteins by altering folding and stability, clearance rate, proteinase resistance, and intrinsic functions, such as receptor binding.[29] It seems that *P. pastoris* is able to modify expressed proteins with N- and O-linked carbohydrates. It is possible that glycosylation at the C-terminal end on Thr^{346} could act in such way to facilitate or alter the receptor binding capacity, enhancing activity. However, the glycosylation would also interfere with the half-life of the protein. In our tumor experiments, Kint3–4 was injected at 48 h.

The importance of glycosylation for plasminogen fragment activity has already been described.[10,27–29] It was observed that the *in vivo* effects of K1–3 are limited to their content of carbohydrates. It was observed also that desialylated angiostatin was ineffective as an inhibitor of tubulogenesis, and it was suggested that the anti-angiogenic effect of angiostatin depends on the contents of sialic acid.

The subcutaneous implantation of a sponge induces a chronic granulomatous response, including intense angiogenesis and the infiltration of inflammatory cells.[30] The vascularization levels on the implanted sponge and in the tumors, assessed by the amount of hemoglobin in the tissues, was significantly reduced, as determined by two methods, colorimetric and by ^{99m}Tc-labeled red blood cells. The sponge-implanted glycosylated K3–4-treated group presented a significant decrease of fibrovascular tissue growth and cellular accumulation, and a lower number of congested blood vessels when compared with the control group.

Leucocytes, in particular, neutrophils and macrophages, are the first cells recruited to local injury.[31] Macrophages mediate angiogenesis through the liberation of substances that act on differentiation, migration, or proliferation of cells, such as growth factors, cytokines, prostaglandins, and proteolytic enzymes.[32,33] Our results showed a significant decrease in macrophage infiltration, that could have mediated the angiostatic effect of K3–4. Angiostatins inhibit neutrophil recruitment.[34] Neutrophils express ATP synthase and angiomotin,[35,36] two angiostatin-receptors that could mediate the effects of Kint3–4 on these cells. Our data showed an inhibition on neutrophil infiltration on the sponge by systemic injection of Kint3–4.

Interestingly, 14 days post-implantation of the melanoma cells, the mortality rate was 50% for the control group, and only one death occurred for the Kint3–4-treated group (n = 20). The treatment protected the animals against this kind of tumor that specifically presents resistance against drugs, radiotherapy, and a high incidence of metastasis.[37] It was demonstrated that some lines of melanoma cells express the integrin cell adhesion receptor $\alpha_v\beta_3$ on their surface.[38] Cross-talking between VEGF, the major angiogenic growth factor, and $\alpha_v\beta_3$ seems to be a critical factor in the regulation of angiogenesis and tumor development.[39] It is probable that one of the mechanisms of action of Kint3–4 involves this integrin, since a significant reduction in the VEGF expression levels was observed after treatment with Kint3–4.

In the present study, we provide evidence that the presence of carbohydrate moieties are of functional importance for the activity of angiostatin analogs. Furthermore, the VEGF expression seems to be an important mechanism in this process. These results expand the current understanding of how angiostatin homologs can interfere with tumor growth, promoting the inhibition of tumor angiogenesis.

Acknowledgments

The authors would like to thank Fapemig, Fapesp, CAPES, and CNPq for financial support.

References

1 Griffioen AW, Molema G. Angiogenesis: Potentials for pharmacologic intervention in the treatment of cancer, cardiovascular diseases, and chronic inflammation. *Pharmacol Rev* 2000; **52**: 237–68.
2 Folkman J. Seminars in medicine of the Beth Israel hospital, Boston: clinical applications of research on angiogenesis. *N Engl J Med* 1995; **333**: 1157–63.
3 Folkman J, Klagsbrun M. Angiogenic factors. *Science* 1987; **235**: 442–7.
4 Colville-Nash PR, Alan CAS, Appleton I, Brown JR, Seed MP, Willoughby DA. The pharmacological modulation of angiogenesis in chronic granulomatous inflammation. *J Pharmacol Exp Ther* 1995; **274**: 1463–72.
5 Montag M, Dyckhoff G, Lohr J *et al.* Angiogenic growth factors in tissue homogenates of HNSCC: expression pattern, prognostic relevance, and interrelationships. *Cancer Sci* 2009; **100**: 1210–8.
6 Klagsbrun M, Moses MA. Molecular angiogenesis. *Chem Biol* 1999; **6**: 217–24.
7 Yanagi K, Onda M, Uchida E. Effect of angiostatin on liver metastasis of pancreatic cancer in hamsters. *Cancer Sci* 2000; **91**: 723–30.
8 Kim CK, Hong SH, Joe YA, Shim B, Lee S, Hong Y. The recombinant kringle domain of urokinase plasminogen activator inhibits *in* vivo malignant glioma growth. *Cancer Sci* 2007; **98**: 253–8.
9 Freeman MR, Schneck FX, Gagnon ML *et al.* Peripheral blood T lymphocytes and lymphocytes infiltrating human cancers express vascular endothelial growth factor: A potential role for T cells in angiogenesis. *Cancer Res* 1995; **55**: 4140–5.
10 Cao Y, Ji RW, Davidson D *et al.* Kringle domains of human angiostatin. *J Biol Chem* 1996; **46**: 29461–7.
11 Weidong-Richard JI, Castelino FJ, Chang Y *et al.* Characterization of kringle domains of angiostatin as antagonists of endothelial cell migration, an important process in angiogenesis. *FASEB J* 1998; **12**: 1731–8.
12 MacDonald NJ, Murad AC, Fogler WE, Lu Y, Sim BKL. The tumor-suppressing activity of angiostatin protein resides within kringles 1 to 3. *Biochem Biophys Res Commun* 1999; **264**: 469–77.
13 O'Reilly MS, Holmgren L, Shing Y *et al.* Angiostatin: a novel angiogenesis inhibitor that mediates the suppression of metastasis by a Lewis lung carcinoma. *Cell* 1994; **79**: 315–28.
14 Tschopp JF, Brust PF, Cregg JM, Stilmam CA, Gingeras TR. Expression of the LacZ gene from two methanol-regulated promoters in *Pichia pastoris*. *Nucleic Acids Res* 1987; **15**: 3859–76.
15 Duman JG, Miele RG, Liang H *et al.* Mannosylation of *Pichia pastoris* cellular and recombinant proteins. *Biotechnol Appl Biochem* 1998; **28**: 39–45.
16 Chen Y, Cino J, Hart G, Freedman D, White C, Komives EA. High protein expression in fermentation of recombinant *Pichia pastoris* by a fed-batch process. *Proc Biochem* 1997; **32**: 107–11.
17 Bailey PJ. Sponge implants as models. *Methods Enzymol* 1988; **162**: 327–34.
18 Hu DE, Hiley CR, Smither RL, Gresham GA, Fan TP. Correlation of 133Xe clearance, blood flow and histology in the rat sponge model for angiogenesis. Further studies with angiogenic modifiers. *Lab Invest* 1995; **72**: 601–10.
19 Machado RD, Santos RA, Andrade SP. Opposing actions of angiotensins on angiogenesis. *Life Sci* 2000; **66**: 67–76.
20 Gomes ML, Oliveira MBN, Bernardo-Filho M. Drug interaction with radiopharmaceuticals: effect on the labeling of red blood cells with technetium-99m and on the bioavailability of radiopharmaceuticals. *Braz Arch Biotechnol* 2002; **45**: 143–9.
21 Barcelos LS, Talvani A, Teixeira A *et al.* Impaired inflammatory angiogenesis, but not leukocyte influx, in mice lacking TNFR1. *J Leuk Biol* 2005; **78**: 352–8.
22 Folkman J. Tumor angiogenesis: therapeutics implications. *N Engl J Med* 1971; **285**: 1182–6.
23 Folkman J. A new family of mediators of tumor angiogenesis. *Cancer Invest* 2001; **19**: 754–5.
24 Shadi PK, Pineda IF. Tumoral angiogenesis: review of the literature. *Cancer Invest* 2008; **26**: 104–8.
25 Sim BKL, O'Reilly MS, Liang H *et al.* A recombinant human angiostatin protein inhibits experimental primary and metastatic cancer. *Cancer Res* 1997; **57**: 1329–34.
26 Zhang AL, Zhang TY, Luo JX *et al.* Constitutive expression of human angiostatin in *Pichia pastoris* by high-density cell culture. *J Ind Microbiol Biotechnol* 2006; **34**: 117–22.
27 Hayes M, Castellino FJ. Carbohydrate of the human plasminogen variants. III. Structure of the O-glycosidically linked oligosaccharide unit. *J Biol Chem* 1979; **254**: 8777–80.
28 Hayes M, Castellino FJ. Carbohydrate of the human plasminogen variants. II. Structure of the asparagine-linked oligosaccharide unit. *J Biol Chem* 1979; **254**: 8772–6.
29 Pirie-Shepherd SR, Stevens RD, Andon NL, Enghild JJ, Pizzo SV. Evidence for a novel O-linked sialylated trisaccharide on Ser-248 of human plasminogen 2. *J Biol Chem* 1997; **272**: 7408–11.
30 Lage AP, Andrade SP. Assessment of angiogenesis and tumor growth in conscious mice by a fluorimetric method. *Microvasc Res* 2000; **59**: 278–85.
31 Butcher EC. Leukocyte-endothelial cell recognition: three (or more) steps to specificity and diversity. *Cell* 1991; **67**: 1033–6.
32 Sunderkotter C, Goebeler M, Shultze-osthoff K, Bhardwaj R, Sorg C. Macrofhage-derived angiogenesis factors. *Pharmacol Ther* 1991; **51**: 195–216.
33 Blair JR, Meng H, Marchese MJ *et al.* Human mast cells stimulate vascular tube formation. *J Clin Invest* 1997; **99**: 2691–700.
34 Benelli R, Morini M, Carrozzino F *et al.* Neutrophils as a key cellular target for angiostatin: implications for regulation of angiogenesis and inflammation. *FASEB J* 2002; **16**: 267–9.

doi: 10.1111/j.1349-7006.2009.01403.x

35 Moser TL, Stack MS, Asplin I *et al.* Angiostatin binds ATP synthase on the surface of human endothelial cells. *Proc Natl Acad Sci U S A* 1999; **96**: 2811–6.
36 Troyanovsky B, Levchenko T, Mansson G, Matvijenko O, Holmgre L. Angiomotin: an angiostatin binding protein that regulates endothelial cell migration and tube formation. *J Cell Biol* 2001; **152**: 1247–54.
37 Rofstad EK, Halsor EF. Vascular endothelial growth factor, interleukin 8, platelet-derived endothelial cell growth factor, and basic fibroblast growth factor promote angiogenesis and metastasis in human melanome xenografts. *Cancer Res* 2000; **60**: 4932–8.
38 Seftor REB, Seftor EA, Gehlsen KR *et al.* Role of the $\alpha_v\beta_3$ integrin in human melanoma cell invasion. *Proc Natl Acad Sci U S A* 1992; **89**: 1557–61.
39 Sarmishtha DE, Razorenova O, McCabe NP, O'Toole T, Jun Q, Byzova TV. VEGF–integrin interplay controls tumor growth and vascularization. *Proc Natl Acad Sci U S A* 2005; **102**: 7589–94.). EAEAYVEF, fused sequence from the AOX1 signal peptide. (b) Partial amino-terminal sequence of plasminogen and recombinant Kint3–4. Amino acids Val^{79} and Thr^{346} are identified.